

Performance Evaluation of a Temperature Control Stage Used on a Semiconductor Gas Sensor 3D Electro-Thermal Model Through Simulink[®]

E.N. Vázquez-Acosta¹, S. Mendoza-Acevedo¹, M.A. Reyes-Barranca¹,
L.M. Flores-Nava¹, J.A. Moreno-Cadenas¹ and J.L. González-Vidal²

¹*CINVESTAV-IPN, Electrical Engineering Department*

²*Universidad Autónoma Del Estado de Hidalgo,
Computing Academic Area*

Mexico

1. Introduction

Actually, the use of CAD-CAE is a widespread activity for design and evaluation purposes. Hence, several programs can be found for simulation and optimization of systems described with 3D graphic representation, giving the morphology of the model (Muñoz et al., 2008). Also, suites can be found that can simulate and prove some kind of controls being described with transfer functions (TFs), differential equations (DE), space states or ASIC models (Goering, 2004).

In general, the design begins creating the file of the solids that describe the geometry of the device through CAD tools and then exported to simulation and analysis environments (multi-physics). Thereafter, the results obtained are used in a multi-domain platform, where more complete results can be obtained for a system in consideration, taking advantage of modules that can link these environments. Now, one should have in mind that if complex dynamic models are to be considered, a serious limitation can be present if two or more variables of the system are mutually dependant. Therefore, it is suggested to export static models. In this case, the role of the modules is centred only to a basic interchange of data between the environments, having not a real and full interaction between the models considered. Then as a recommendation, it is convenient to include all the possible dynamics in the exported model, even as a part of it or as an external issue, such that the dynamic simulation can give more precise results. On the other hand, when a dynamic simulation is done based on a static model, there could be a dramatic increase in simulation time since a call to the static exported model will be done at each simulation time step. For instance, if a simulation is specified for a 1s lapse with 1ms steps, the exported model will be called 1000 times.

The particular case exposed in this paper is the analysis of a coupled thermo-electrical model designed to operate a micro hotplate (MHP) with a temperature control circuit, used

in an integrated semiconductor gas sensor (SGS). The analysis should consider that the MHP will be physically located in a thin membrane created with MEMS technology. The complexity of this system is rather high since a thermo-electrical coupling must exist among devices that operate as a heat source and the different layers affected by the generated heat. Specifically, the case here studied treats the Joule Effect applied to the polysilicon material used in integrated circuits. Thus, it is necessary to combine somehow the analysis programs to obtain the required electro-thermal simulation results and to verify if the expected performance, i.e. temperature variation in time, is correct.

2. Description of the system

A SGS was designed based on layers available in standard CMOS technology, having two polysilicon layers and two metal layers. The layout of the prototype is shown in Fig. 1.

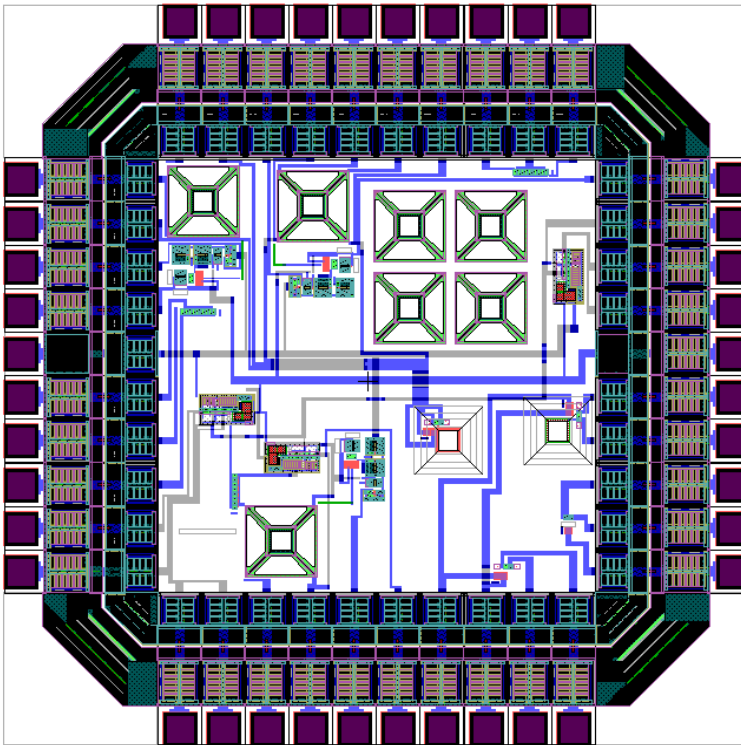


Fig. 1. Layout of the gas sensor prototype.

One advantage in using this kind of technology is its compatibility with MEMS micromachining processes made with anisotropic etching solutions as tetramethylammonium hydroxide (TMAH), resulting in a preferential etching of the silicon substrate. This way, a very thin membrane is obtained containing the MHP (Fedder, 2005). The layout of the integrated sensor circuit is shown in Fig. 2, where the different blocks implemented for the system, are identified.

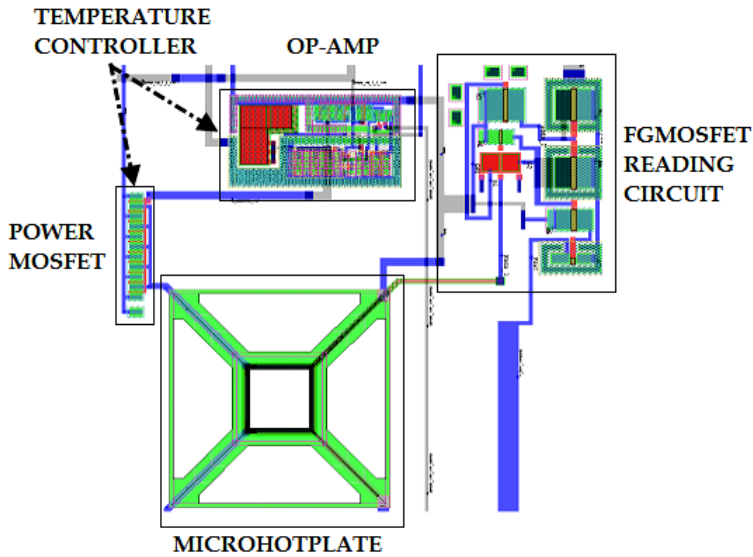


Fig. 2. Layout of the integrated gas sensor system.

This kind of gas sensor can be fabricated starting with a silicon substrate and includes a micro hotplate (MHP), whose structure stands as a mechanical support for the layers contained in the thin membrane (SiO₂/Polysilicon/SiO₂/Polysilicon/Metal Oxide). The thin film located above all these layers is a sensitive metal oxide layer that senses the gaseous species to be detected. Besides, the main purpose of the membrane is to isolate the heat generated in that zone and to uniformly distribute the temperature in the thin membrane.

The size of the MHP is 80µm × 80µm and will be suspended by four arms over the microcavity obtained after a bulk micromachining post-process usual in MEMS technology, giving an effective thermal isolation from the substrate. This way, the thermal mass of the MHP is reduced and as a consequence, its thermal inertia is decreased. Therefore, it is easy to attain an operation temperature range between 250°C and 350°C with low voltages applied (< 2.5V). This temperature promotes the chemical reaction between the thin metal oxide layer and the gas species (Afridi et al., 2002). Also, the MHP contains a micro temperature sensor (TS) and a microheater (MH) that is biased to raise its temperature due to the Joule Effect. Both will be fabricated with polysilicon and the proposed configuration is shown in Fig. 3.

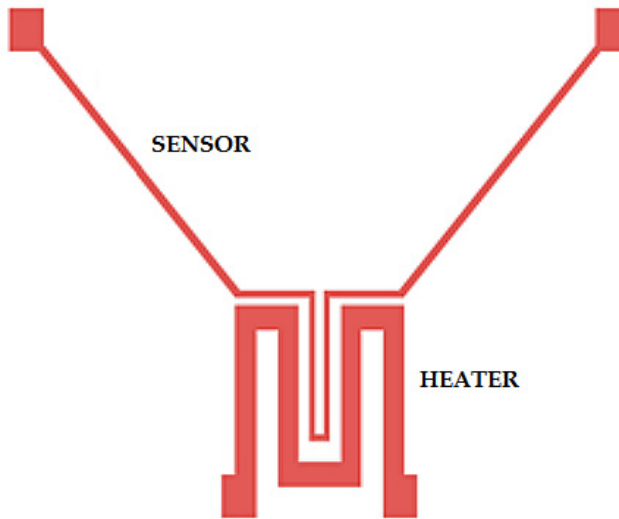


Fig. 3. Geometry of the microheater resistor and the temperature sensor.

When implemented as a resistor, polysilicon increases its resistance value proportionally with an associated temperature rise. This property is named Thermal Coefficient of Resistance (TCR) (Cerda et al., 2006). The relation of the resistance value with a temperature change is expressed with the following equation:

$$\frac{R - R_0}{R_0} = TCR(T - T_0) \quad (1)$$

where T_0 is room temperature and R_0 is the resistance value at room temperature. TCR and R_0 can be experimentally determined. If the relation between temperature and resistance is known, it can be conveniently used to design a temperature control circuit if a constant current is passed through TS. If a DC voltage is applied across the microheater terminals, the resistance value of polysilicon increases as predicted by equation (1). Fig. 4 shows the variation of the resistance of TS and MH as a function of temperature from where TCR can be obtained.

TCR property sets a problem hard to solve from the simulation point of view when using traditional methods or programs like SPICE, since there is no possibility to consider at the same time the Joule Effect and the electro-thermal coupling between MH and TS. Also, it is difficult to properly consider the thermal inertia of the MHP's thermal mass using electrical simulators.

From Fig. 3, it is easy to deduce that the thermal coupling between the temperature sensor and the microheater is possible because of their proximity, so the fact that TS follows the temperature changes in MH can be used favourably. As it is well known, the thermal coupling behaviour depends on the properties of the materials used. For the structure here analysed, the materials involved are crystalline silicon, polysilicon, silicon dioxide and aluminium.

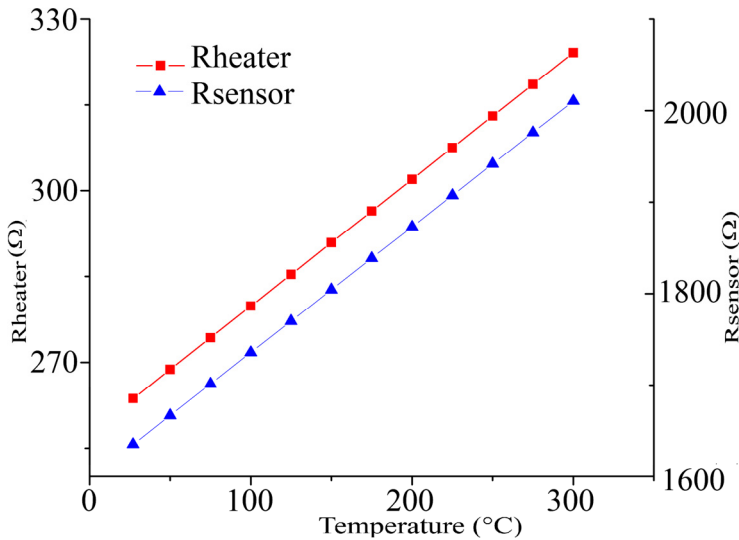


Fig. 4. MH and MS resistance value as a function of temperature.

Based on the later and the geometry drawn (Fig. 3), then the system will have a particular thermal response time for heating and cooling of the MHP. This is precisely the performance that is desired to be evaluated. Given the above background, the objectives of this work are: a) to propose a simulation and analysis strategy to find the dynamic behaviour of the model of the MHP driven by a temperature control circuit, based on the results obtained from the electro-thermal analysis, and b) to optimize the computing resources and simulation time. If the results are the expected, then the system can be fabricated with confidence. The following sections establish the proposed methodology.

3. Electro-thermal model

3.1 Simulation based on finite elements

Using specialized CAD software, a 3D solid model was created in order to propose the geometry of the structure needed for the electro-thermal analysis and simulation. This geometry should include the microcavity that is supposed to be made with the anisotropic etching after the fabrication of the chip. Once the geometry is finished, it can be exported to a multi-physics platform and proper sub-domains were assigned as well as boundary conditions (DC conductive media and heat transfer) to perform the analysis of the electro-thermal model. Also, to assure convergence with the finite elements analysis, a convenient mesh density should be selected. The analysis was made using an applied voltage sweep from 1V to 3V with 0.2V steps. The result is shown in Fig. 5, where the electro-thermal behaviour of the 3D geometric model of the gas sensor can be seen after the analysis with finite elements. Here it is confirmed that the heat is focused at the MHP as a result of the micromachining specified before. It should be noted that although the TS is not biased, it will have the same temperature induced by Joule Effect in the MH as a consequence of heat transfer by conduction across the silicon dioxide between them.

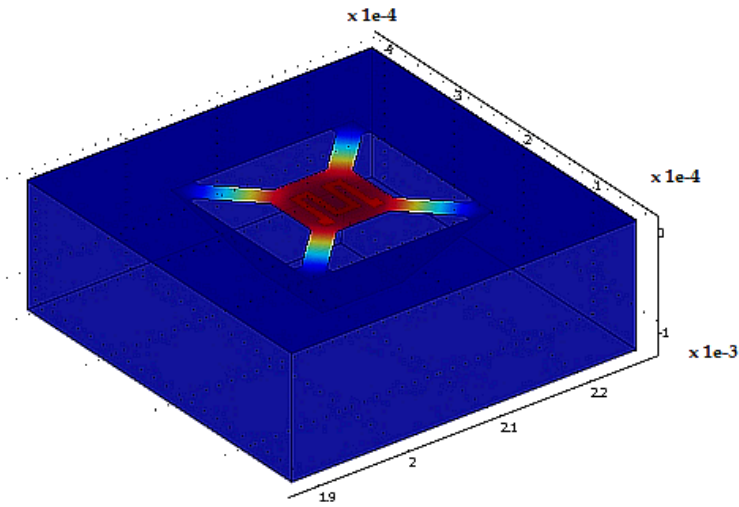


Fig. 5. 3D exported model from AutoCAD® after simulated with COMSOL Multiphysics®.

Using this same platform (multi-physics), the thermal response as a function of time having the applied voltage as a parameter was also obtained. Figs. 6 and 7 show the results for heating and cooling, respectively and it should be mentioned that a different response will be obtained for different geometries of MH and TS. This behaviour follows the change in resistance of polysilicon predicted by equation (1).

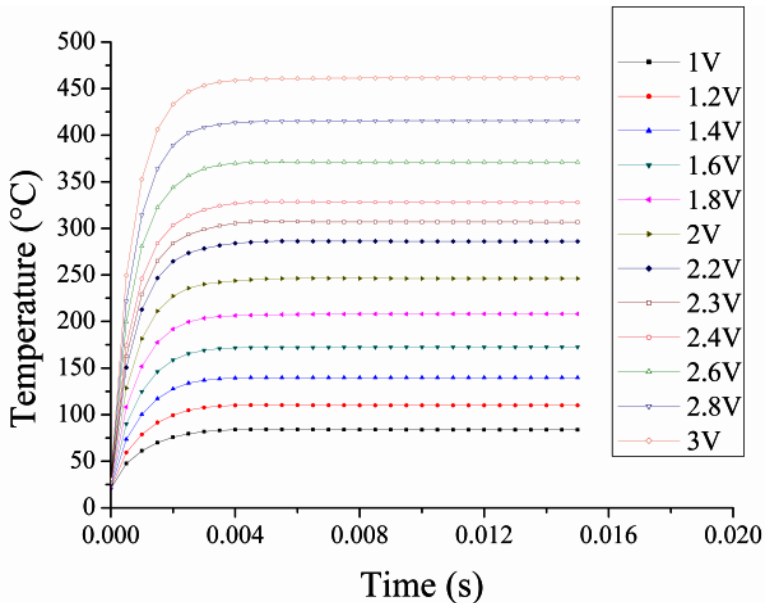


Fig. 6. MH heating response with applied voltage as a parameter.

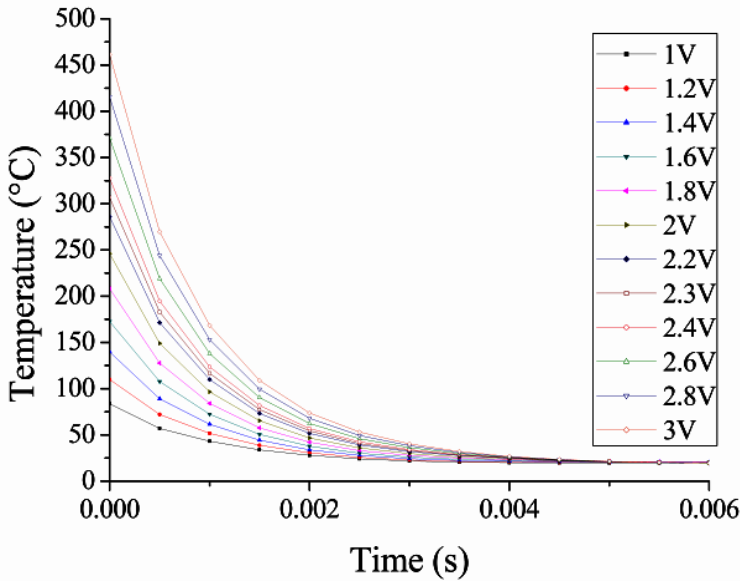


Fig. 7. MH cooling response with applied voltage as a parameter.

3.2 Simulation of the static model with the transfer function at the output

The model created in the multi-physics environment can be exported to a multi-domain environment using the existing modules specially created to link different software suits. Once the model is exported, one arbitrary exciting input and several reading outputs can be declared. In the case here exposed, the input is described as the voltage applied to MH. The value (or even the waveform) of this voltage can be modified along the simulation process in the multi-domain software. This is not possible to do with the multi-physics program. One of the outputs is declared as the reading of the temperature reached by MHP. The typical TCR of polysilicon can be easily calculated from this temperature reading.

Regardless of the possibilities and advantages that linking modules have, the model presents limitations when it is exported due to the mutual dependence of the variables as described by the electro-thermal coupling, therefore it is exported only as a static model.

Due to the above reason, transfer functions (TFs) must be added at the output of the simulation block of the exported system to consider dynamic features of the model. This makes possible to emulate the dynamic behaviour while heating or cooling, following the results obtained in Figs. 6 and 7. From now on, this model will be named as the exported model. For the case here reported, the TFs of interest can be obtained after making a series of heating and cooling cycles using the voltage range specified in Figs. 6 and 7. With the results obtained, an expression that nearly fits with the heating and cooling curves can be extrapolated. This can be done either with computational methods or by trial and error. Selection of the order of the expression of the TFs highly depends on the response of the system to a step input signal and to the desired accuracy. Since the system here analysed has no over damping, using a first order TF will simplify the task (Ogata, 1999).

The simplest expressions that fit approximately with the dynamics of the original system are the following:

- Cooling TF:

$$G_c(s) = \frac{1}{0.00077s + 1} \quad (2)$$

- Heating TF:

$$G_h(s) = \frac{1}{0.000095s + 1} \quad (3)$$

Fig. 8 shows the result after the simulation of the static model, together with the deduced TFs output when a voltage pulse was applied to the MH.

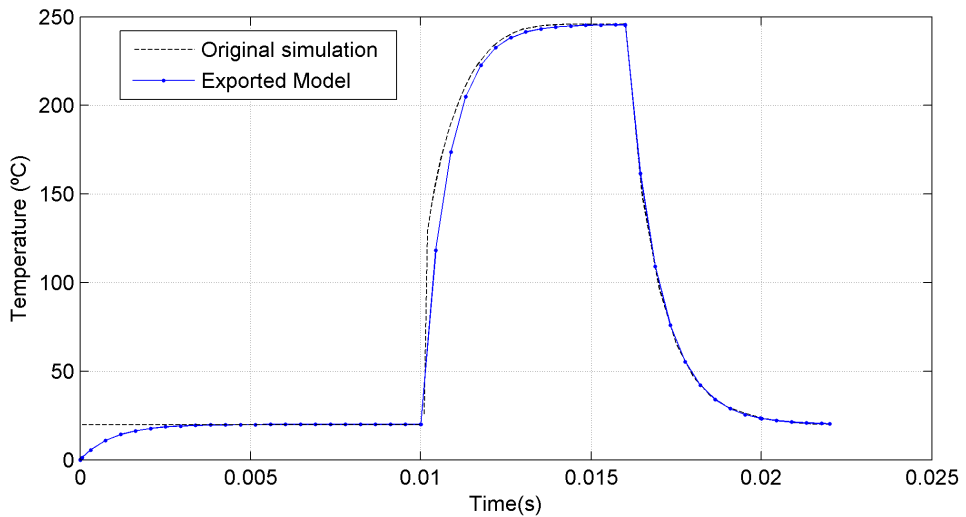


Fig. 8. Output of the static model when excited with an input step signal (continuous line) and the transfer function deduced from Figs. 6 and 7 (dashed line).

Once these TFs are included it is possible to apply arbitrary inputs to the system and read their corresponding dynamic outputs storing them as variables of the multi-domain software, with Simulink® of Matlab®, for instance. Also, it is possible to add and simulate some kind of temperature control block together with a signal processing or ASIC circuit. The later is not possible to do within the environment from where the created model was exported. Using the approximation with TFs it is possible to use certain blocks that call the exported model only when there are abrupt changes in the system's input. This helps to decrease the computing processing time (Hsu, 2002). Therefore, the suggested block diagram of the model that can be simulated with this alternative is shown in Fig. 9. This figure shows the block of the simulated electro-thermal system (COMSOL Subsystem), a signal generator block (Signal Builder), a block that calls the exported static model simulation (Pulsed COMSOL Sim), having the task to evaluate the model only when a

change at the input signal is detected, saving this way time and computational resources. Here, existing modules that detect signal changes (Detect Change) are used together with a Boolean converter and a module that evaluates the exported model (COMSOL Triggered Simulation) followed by a Hold block that keeps the output value until there is a change at the input signal. All these modules are contained in the library of the multi-domain platform. Other supporting blocks included in Simulink® are a temperature unit converter (from K to °C), the Dynamic Adjust block that includes the heating and cooling TFs deduced before, and finally a block that displays the output waveform (Scope).

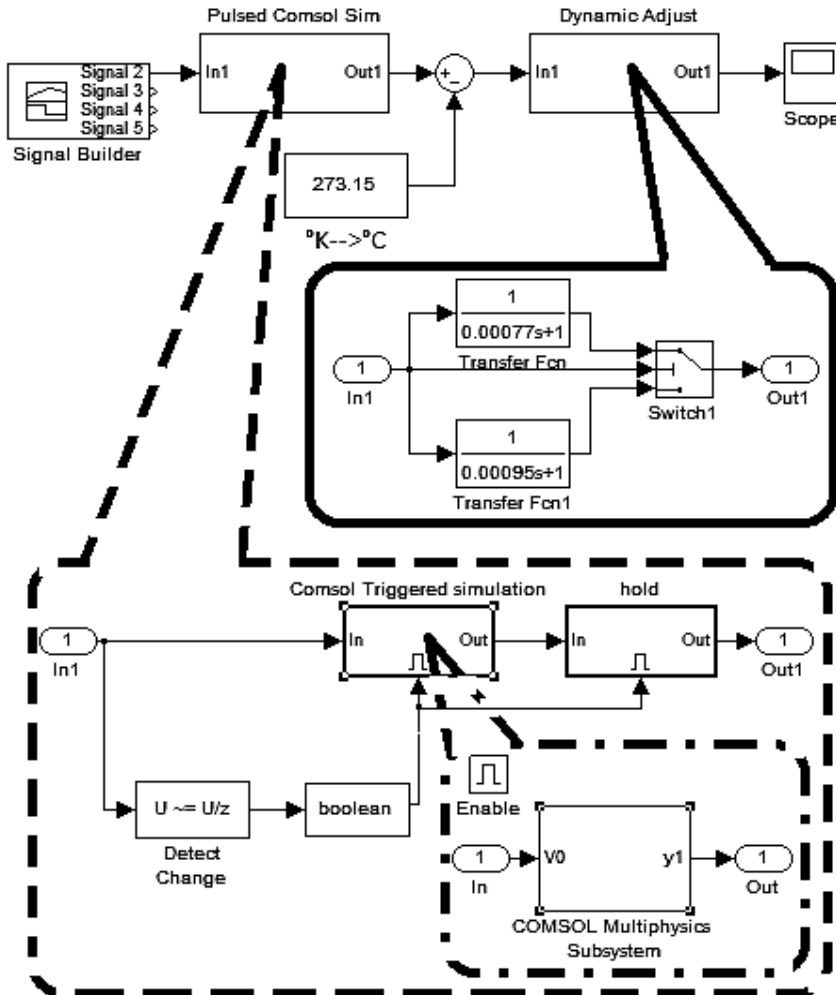


Fig. 9. Block diagram of Simulink® for the pulsed simulation.

3.3 Simulation with the approximated equation and transfer functions

The model illustrated in Fig. 9 presents great performance advantages if the applied inputs present abrupt changes in time like step signals. However it could be extremely slow if input signals have no abrupt changes during time like ramps or sine waveforms. So, if signals continuously changing in time are to be used, a more useful method to apply is based on the substitution of the block that calls the model (illustrated in Fig. 9), with an approximated equation that closely follows the temperature dependence of MH to the applied DC voltage, as obtained in the multi-physics platform. The kind of equation can be arbitrarily chosen while the parameters of it should be adjusted using the data obtained from the simulation of the exported model. Again, this can be done with the help of computational regression methods or by trial and error. Care should be taken to assure that the equation used is valid at least within the voltage sweep range of interest. The equation found for the case here presented is the following:

$$f(x) = 64x^{(1.938 - 0.0605x)} + 20 \quad (4)$$

where $f(x)$ is the temperature output in K and x is the voltage applied to the MH in the exported model. Fig. 10 shows good agreement between the curve obtained after the static simulation of the exported model and the plot of equation (4).

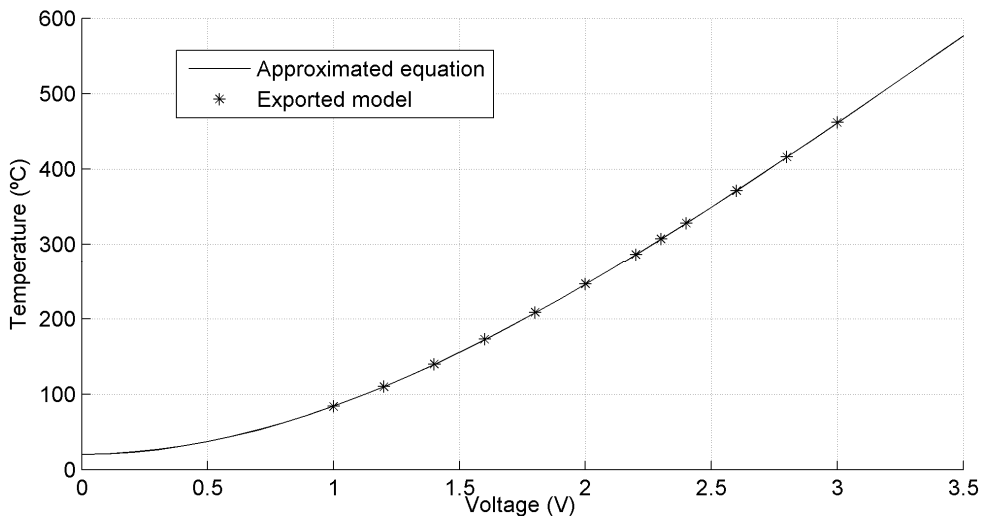


Fig. 10. Comparison between the static model and Eq. (4).

Therefore, this different alternative can be used properly in the desired dynamic simulation of the model. Once the approximated equation is obtained, it can be integrated into the simulation model instead of the module that invokes the pulsed exported model, using a function block as is shown in Fig. 11. Then, three options for the model simulation were presented: the exported model (3.1), the exported static model (3.2) and the approximated model (3.3). A series of simulations can be done to compare performance, validate the models and make a convenient choice among these methods. At first glance, a MH temperature range of 172.6 °C - 327.8°C

(corresponding to a voltage range of $2V \pm 0.42V$) was used. The first test was done using a pulse train having arbitrary widths and magnitudes. The results are shown in Fig. 12.

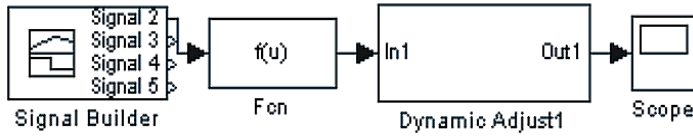


Fig. 11. Model with the approximated equation.

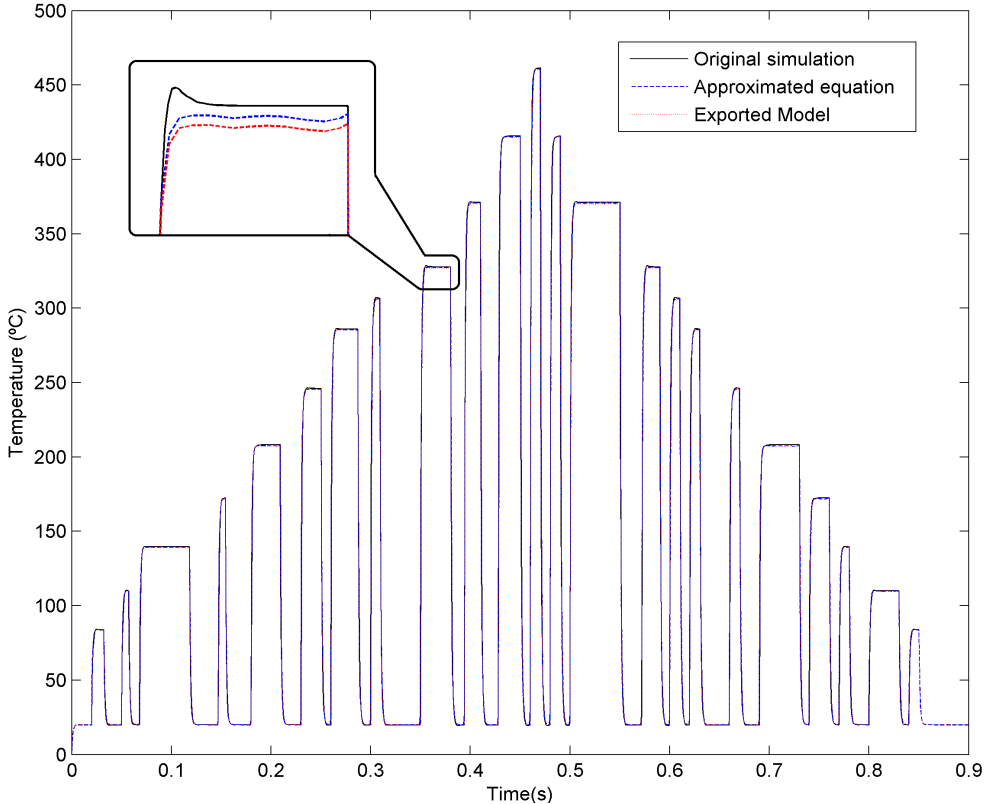


Fig. 12. Results from the simulation using the three analysing alternatives proposed, with an arbitrary pulse train as input.

As shown in Fig. 12, the three curves are quite similar among them. Deviation of methods 3.2 and 3.3 compared with 3.1 is only 0.22% in the worst case, meaning a variation of $1^{\circ}C$ each $461.4^{\circ}C$. Hence it can be concluded that these options give similar results such that each of them can be used with confidence in the voltage range studied. However, it should be remembered that the exported model is limited to tests with simple on-off temperature controls and/or for abrupt inputs or with almost no changes in time. Otherwise, if inputs like a ramp or a sine waveforms are used, for instance, the static model will be invoked at each

simulation step declared, increasing considerably the processing time. Since the objective is to optimize the simulation procedure, method 3.2 will be discarded from now on and only the original model (3.1) and the last one (3.3) will be considered in the following analyses. Comparative simulations between these two last methods were made, using the results of the original model obtained in the multi-physics environment and those obtained using the approximated model in the multi-domain platform. The results are shown in Figs. 13-15.

With these last results using arbitrary waveforms as input to the MH, heating and cooling can be effectively evaluated considering also heat dissipation due to the environment that is surrounding the system.

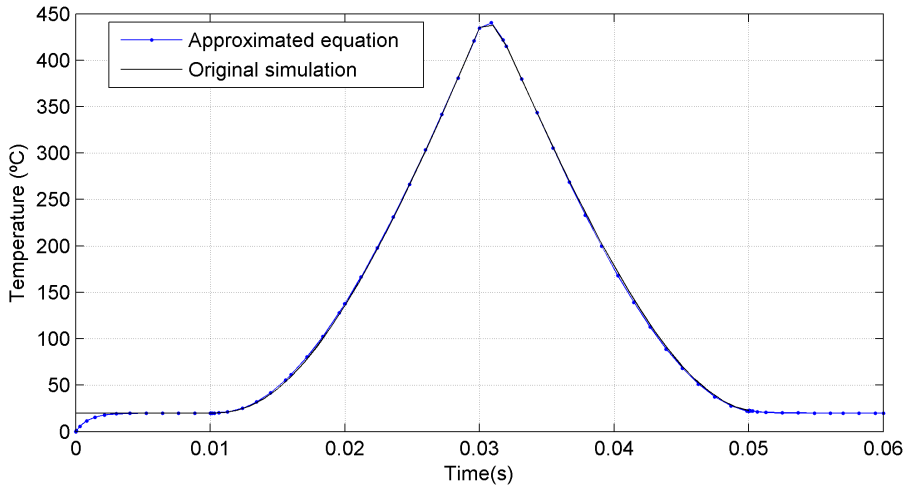


Fig. 13. Comparative with a saw tooth input signal.

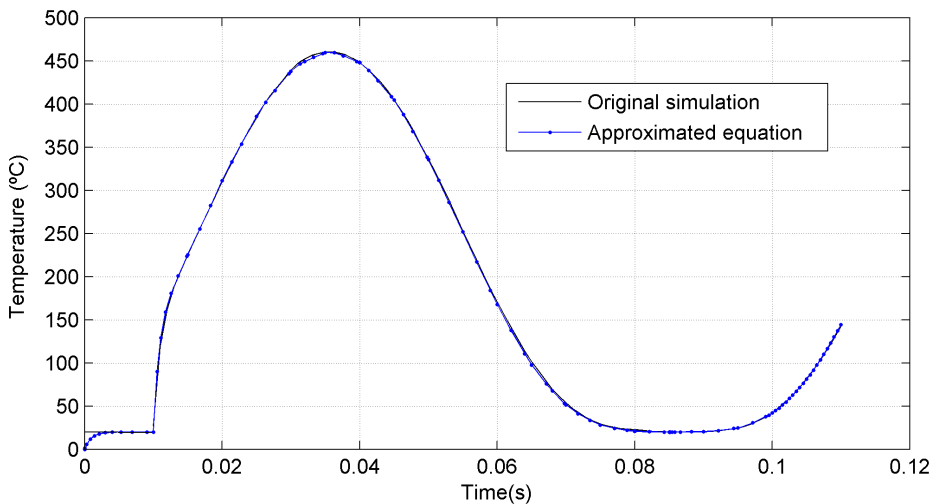


Fig. 14. Comparative with a sine waveform with a 3V amplitude and 10Hz frequency.

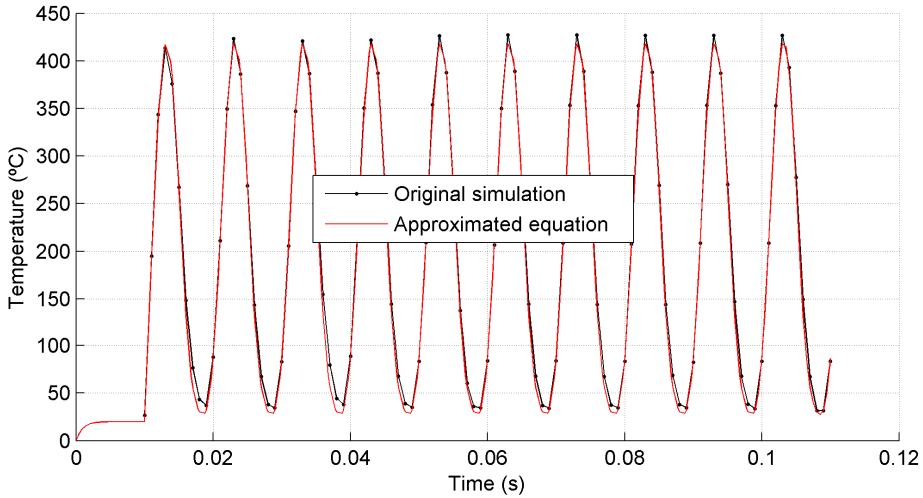


Fig. 15. Comparative with a sine waveform with a 3V amplitude and 100Hz frequency.

Near to real operating conditions can be considered this way. Also, it should be noted that the initial temperature considered in the multi-physics simulation is 20°C, as established in the boundary conditions, but the simulation results obtained with the approximated model (see Fig. 11) begin at 0°C, as shown in Fig. 16.

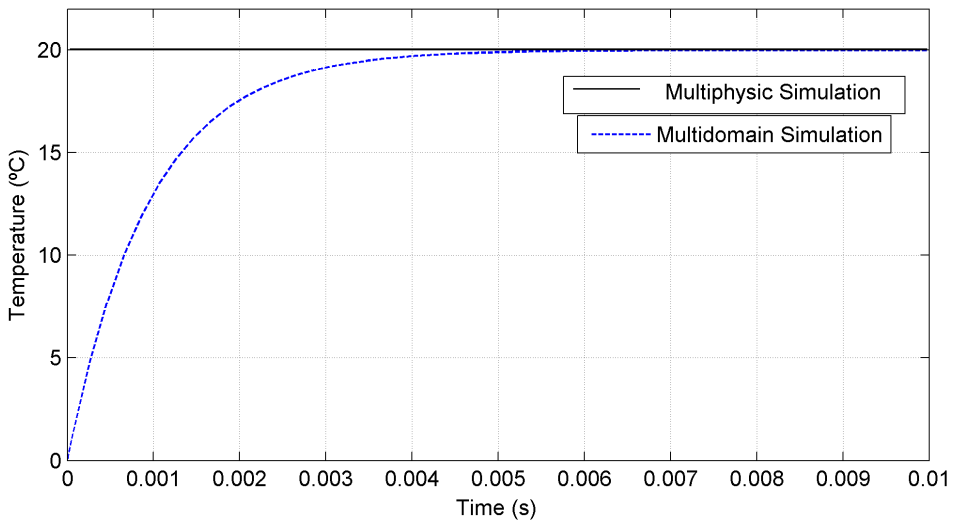


Fig. 16. Stabilization time to room temperature.

So in order to compare at same temperature points, the multi-domain simulation is first allowed to stabilize at 20°C, then the input signal is applied. Therefore, the considered waveform is started after 0.01s although the temperature stabilization time is shorter as is

seen in Fig.16. Taking the temperature stabilization to times shorter than 0.001s may affect the simulation dynamics at the beginning.

Based on the above, it may be concluded that the outlined strategies have good performance and therefore they can be used to continue with the system design. Now the temperature control circuit will be included for the next analyses. So, after the validation of the models, the following step is to prove a temperature control, either using blocks from the library of the platform or using integration modules with other simulation programs. Once this is made, the designer can have a global idea about the performance of the system with the possibility to optimize the design.

4. Model of the temperature control system and simulation

For the temperature control of the micro hotplate obtained with post-processes compatible with CMOS technology described before, an analogue proportional control based on an operational amplifier (OP-AMP) is proposed (Barrentino et al., 2004). The schematic used for the basic simulations of the system is shown in Fig. 17.

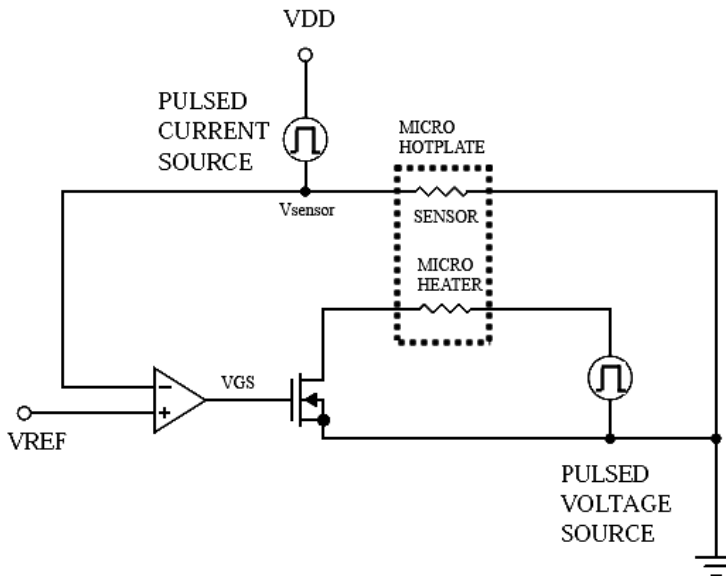


Fig. 17. Schematic of the temperature control circuit.

From the mentioned electro-thermal characteristics of polysilicon, MH and TS can be used as part of a temperature control circuit. When the temperature sensor is connected as a feedback from the output to the input of the operational amplifier, the voltage drop in it is compared with a reference voltage (V_{REF}). If the voltage difference between both inputs is zero, a power MOS transistor used as a switch connected at the output of the OP-AMP, will interrupt the biasing to the MH. A regulated current source applying pulses with constant amplitude should be used to bias TS (note that this does not cause Joule Effect to TS). Due to heat transmission by conduction, the resistance in the TS will increase (see Fig. 4) and its voltage drop will be modified. This property makes feasible to apply the TS in a temperature control circuit. On the other hand, the MH should be biased with a pulsed voltage source to heat the MHP. The magnitude of the pulse depends on the desired temperature. Besides, a pulsed stimulus will help to reduce the power consumption of the system.

Hence, when the reference voltage is higher than the feedback voltage drop, the output of the OP-AMP is high making the MOS transistor to conduct allowing a current flow through the MH. So, due to Joule Effect the temperature will gradually rise from room temperature up to a temperature established by the applied voltage, V_{REF} . At the same time the TS will follow the MH's temperature, changing also the voltage drop on it. At the moment when both voltages are equal, the OP-AMP output will go low turning off the MOS transistor and heating will stop. This cycle will be repeated according to the heating and cooling dynamic behaviour of the microheater, operating around the desired temperature. It is expected that the MH will keep this temperature until the set point is modified if a different temperature target within the physical and mechanical limits of the MHP is desired. Next, to ease the dynamic analysis of the controlling circuit, an equivalent circuit was used to consider the thermal coupling between the heater and the sensor as well as the time constant of the electro-thermal system. The MH was replaced with a voltage controlled voltage source and the TS with an RC circuit, where R and C are the thermal resistance and thermal capacitance of polysilicon, respectively. The corresponding time constant of this circuit should be consistent with the thermal behaviour of the 3D model of the MH considered.

From the finite element analysis made above, different time constants resulted for heating and for cooling (see Figs. 6 and 7). That is the reason why the equivalent circuit shown in Fig. 18 has two resistance elements corresponding to each value. The magnitude of R for heating is 770Ω and 950Ω for cooling. The capacitance value used to fit with each time constants is $1 \mu\text{F}$; the circuit was biased with $V_{DD}=1.5\text{V}$. The transient behaviour of the system can be evaluated using the circuit shown in Fig. 18. The voltage drop in C is equivalent to the temperature reached by the system and is also the feedback voltage of the OP-AMP. Finally, the MOS transistor switch is replaced by two MOS transistors (PMOS and NMOS) to handle charge and discharge (heating and cooling, respectively) of the capacitor, as the output of the OP-AMP goes high or low. This is the reason why two resistors are used, so heating and cooling can be considered. The results of the transient analysis of the circuit show that there will be control over the current flow of the microheater until the voltage drop on TS reaches the reference voltage (1V for the case illustrated in Fig. 19). As soon as the voltage at the gate of the MOS transistor, V_{GS} , equals the reference voltage, then biasing of the microheater stops. According to the cooling dynamics of the microheater, bias will be switching on and off to hold the temperature around the operating point as can be seen in Fig. 19.

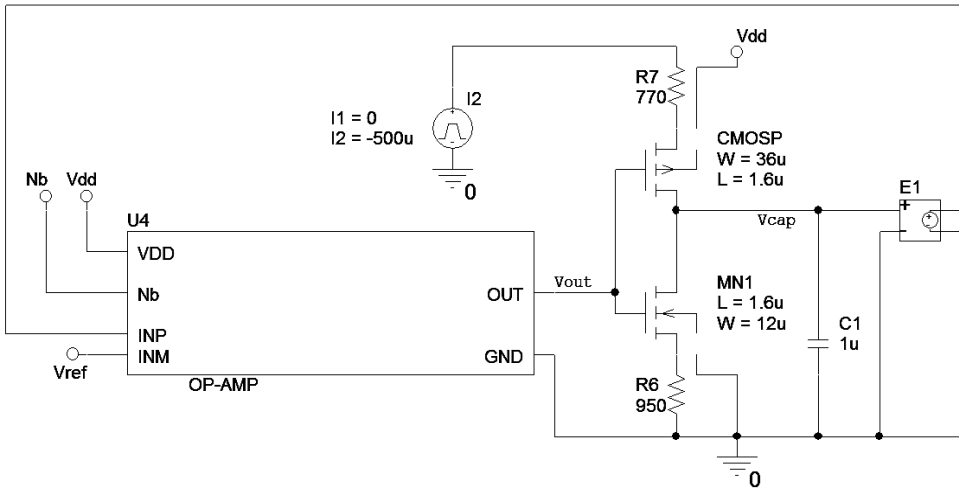


Fig. 18. Equivalent circuit of the temperature control circuit.

In order to have a complete analysis of the performance of the circuit, it was simulated also in SPICE with a temperature sweep (27°C to 300°C) applied to MH and TS and keeping all other circuit components at room temperature (27°C). The result is shown in Fig. 20, where it can be seen that the output of the OP-AMP goes low when the set point (1V) is reached. This is the expected behaviour for the control circuit but it should be noted that this simulation is independent to time, so it is not a dynamic analysis. Then, from Figs. 19 and 20 it can be considered, as a first approximation, that the system behaves as it should even for heating or cooling of MH.

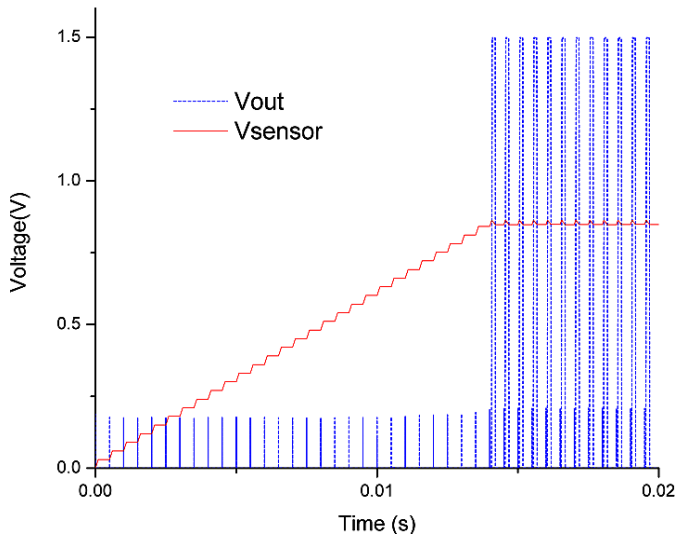


Fig. 19. Simulation results from the equivalent circuit shown in fig. 18 using SPICE.

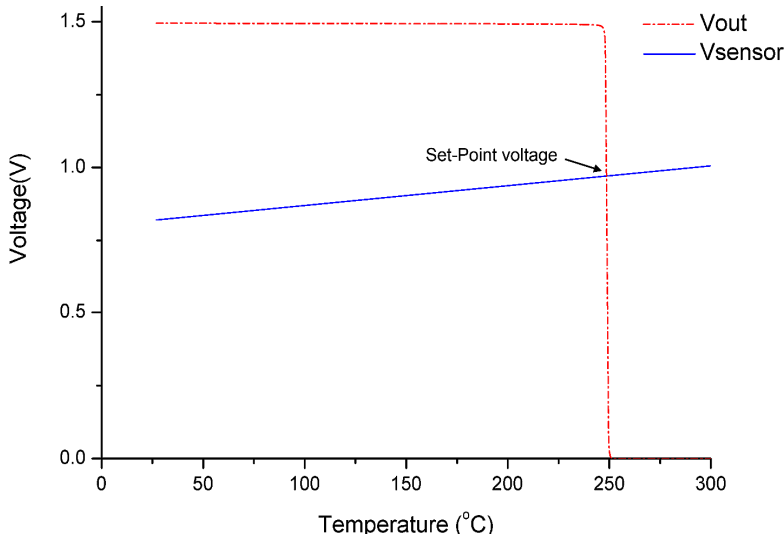


Fig. 20. Output of the OP-AMP when a temperature sweep is applied to MH and TS.

5. Simulation using Simulink®

It is important to remark that simulating the control circuit with SPICE presents a limitation since it is not possible to directly model the electro-thermal coupling between the microheater and the temperature sensor. Therefore, the simulation result shown in Fig. 19 does not take into account the heat transfer by conduction. As a consequence, the result obtained in that simulation is not fully consistent with the real behaviour of the system. Then to consider the thermal coupling, other tools are required such that an analysis of the system with conditions near to real can be done as a function of the elements and materials used in the electro-thermal system together with the temperature control circuit.

To simulate the dynamic performance of the circuit upon temperature changes over the MHP, it is necessary to follow a strategy that can take the SPICE model to a dynamic environment including random temperature changes in time. This is not a task that can be done exclusively with SPICE. Simulink® can help to achieve this using the SLPS integrating block and handling the electro-thermal feature of the micro hotplate with function blocks. It should be mentioned that the SLPS block allows interaction between models of the circuits described in SPICE and models found in Simulink®, whether they were designed using this platform or imported from some other environment. To make use of the SLPS block, it should be initialized from Matlab® as recommended by the supplier; once this is done functional blocks will be available in the library of Simulink. There, the desired interacting block can be loaded identifying the name of the circuit described in SPICE and the respective inputs and outputs are then selected. On one side, inputs are previously defined in SPICE as input voltage sources of the circuit, and on the other side, the output ports will drive a component or device simulated with SPICE. Nevertheless, the SLPS block has only one input and one output, both multiplexed since the use of MUX or DEMUX blocks must be used in Simulink® to read more than one input or output if this is the case.

Based on this, the circuit described with SPICE must be modified to work properly with the SLPS block. The proposal here reported gives good results if the temperature sensor resistor and its biasing current supply are eliminated, keeping only the OP-AMP, the MOS transistor switch and the microheater resistor, connecting them to voltage sources in SPICE, as is shown in Fig. 21. With this procedure, the SLPS block uses the simulation profile of SPICE and the output files from the corresponding simulation. The power supplies and the MHP model are external to this block in the Simulink® environment. The simulation will contain every element of the micro hotplate and the temperature control circuit must be adjusted to the previous simulation conditions. The values used in the voltage sources are shown in Table 1. They correspond to requirements like low power consumption, $V_{DD}=1.5V$, a compensation voltage for the OP-AMP of $V_{nb}=0.6V$, a feeding voltage for the MH of $V_{trans}=3V$ and a reference voltage corresponding to $250^{\circ}C$, $V_{REF}=0.971V$.

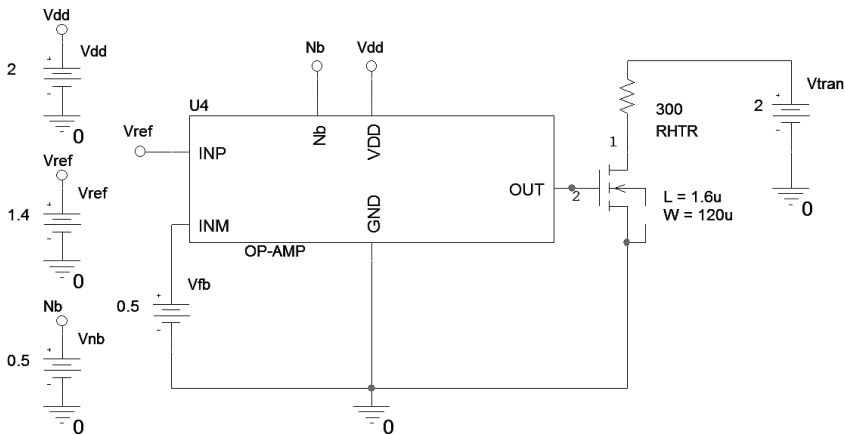


Fig. 21. SPICE circuit description for simulation with Simulink®.

6. Results and discussion

First, a simulation was done for an on-off control circuit using the function blocks that consider the electro-thermal model including TS and MH with their respective features like thermal coupling, temperature sensor morphology and its biasing current. This simulation helps to prove the models developed for the MHP and the dynamic performance. Fig. 22 shows the configuration used for this purpose. On the other hand, it is possible to use the SLPS block with the simulation profile together with the output files from SPICE to integrate the results from both simulations within only one process. Using the conditions specified in Table 1, the performance of the proposed control circuit can be evaluated.

Variable Values	
Vdd	1.5V
Vnd	0.6V
Vrans	3V
VREF	0.971V

Table 1. Variable values for simulation.

The block diagram is shown in Fig. 24. Random temperature variation affecting the system can be included in the descriptions shown in Figs. 22 and 24 with the objective to observe the response of the control circuit of the gas sensor system when temperature perturbations are added to the surrounding environment. Hence, any external factor that should alter the operating temperature of MHP will be considered.

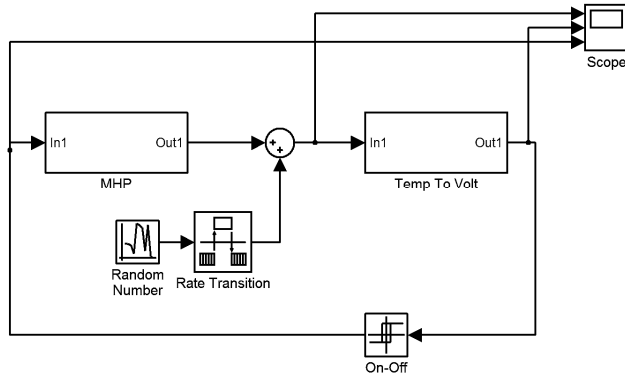


Fig. 22. On-Off Configuration.

When the diagram shown in Fig.22 is simulated, a plot of the temperature variation across time can be obtained showing the behaviour of the MHP connected to a temperature control. As soon as the MH reaches a given temperature established with the set point, the control system maintains this temperature as close as possible, through the control of the switch transistor with the output of the OP-AMP. Fig. 23 shows that a rather good temperature control is achieved around 250°C, as the proposed operating temperature.

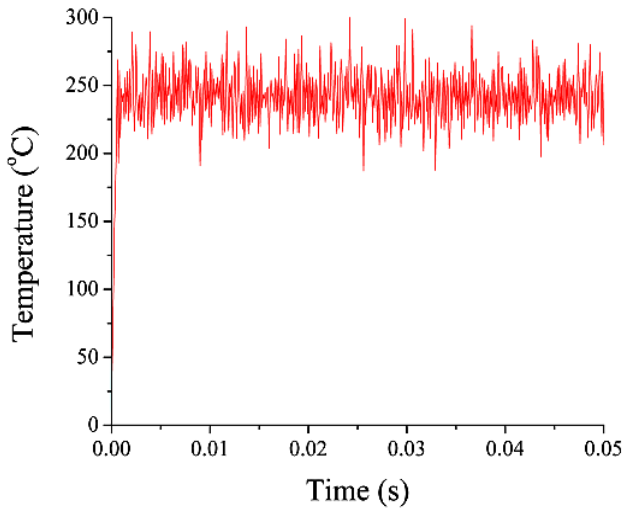


Fig. 23. Simulated operating temperature of MHP without SLPS and considering random temperature variations.

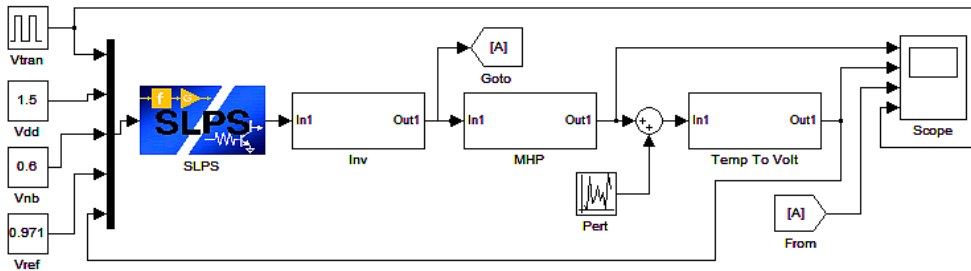


Fig. 24. Block diagram using Simulink®.

Later, including the SLPS block as indicated in Fig. 24, the same simulation as before was made and the results are similar to those presented in Fig. 23, oscillating too around 250°C, as can be seen in Fig. 25.

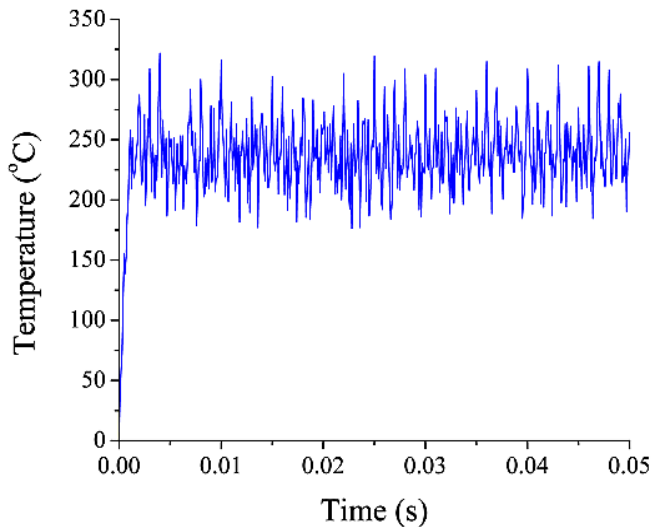


Fig. 25. Simulated operating temperature of MHP with the SLPS block included, considering random temperature variations.

Obviously the oscillations shown in Figs. 23 and Fig. 25 are different but there are two reasons for this: first, since random temperature variations were used, every simulation will generate different values that are not coincident each other; second, it should be remembered that the circuit simulated using SLPS, considered a pulsed current driver to decrease power consumption. Although it can be considered that real external temperature variations will not have such abrupt and rapid transitions, the temperature control circuit is able to hold the temperature around the desired set point. After these simulations, it can be said that the objectives of this study were achieved, this is, a proper design of a temperature control for the MHP that considers the electro-thermal coupling of the materials used for the SGS and with a particular geometry. As it was shown, both strategies can be used for evaluation and validation since they give reasonable results

either using a simple on-off control block or with a more elaborate control circuit based on an OP-AMP. If a rapid evaluation of the performance is desired, a simple block with Simulink® can be used, which can give an approximated idea if the system is giving the expected results. This can be the basis for a more complete analysis using a more complex temperature control circuit based in the SLPS integrating block of Simulink®. It should be remembered that a single geometry for the MH and TS was studied in this work, but depending on the results obtained in the multi-physics environment, it should be optimized also to avoid heat concentration on borders and corners of MH that will damage the structure and to minimize as well the voltage applied in order to reach a given operating temperature. Besides, as this can be a time consuming process until a highly optimized design is obtained, it is convenient to have a strategy that helps to readily have the system design that can be fabricated with no fatal consequences. Finally, it was possible to couple different software environments to complete in short time the electro-thermal analysis of a 3D structure with its temperature control circuit included and with no huge computational resources. For example, the simulation performed to obtain the results shown in Fig. 12 took approximately from 4 to 6 hours to finish using a laptop loaded with a 3D solids engineering and analysis software based on finite elements, to generate the model. On the other hand, the simulation of the exported static model shown in Fig. 9, took from 1 to 2 hours to give the same results in the same machine. Finally, the approximated model illustrated in Fig. 11, gave also the same results in as much as 15 minutes. This is a dramatic difference and the criteria used in the present analysis can be used in turn, to extrapolate to other kind of systems or analyses.

7. Conclusions

The simulation with approximated models have excellent results in repetitive tests, since they reduce the use of hardware requirements, optimize simulation time and avoid interconnection as well as related problems among software programs. There may be cases in which models created in a multi-physics environment can be exported to Simulink® in a dynamic fashion, but the risk of no convergence may be present if there are inconvenient or unexpected changes in the simulation time step. In this case, the exported model will not be useful and the evaluation of the control stage cannot be done. Regardless the approximated model method is faster and allows driving signals as ramps or sine waveforms, results will depend on the equation accuracy and its range of validity. Therefore, the simulation option using approximated models can be the solution to accelerate tests and to apply controls to the model. Also, it can be considered a useful methodology for those users working with rather complex models and having no high capacity resources. However, it is recommended to always verify, if possible, the results with the original program and to try to find models using higher order TFs. There is no doubt that the CAD resources definitely support developing and design activities. Nevertheless, sometimes they may be limited to specific tasks so it is necessary to assess and to explore different alternatives. For some cases, partial results thrown by simulations can be considered good enough, but it will be preferable to have wide information about the behaviour of a system. Coupling compatible simulation environments can be a reliable strategy as was demonstrated for the case presented in this work, where satisfactory results were obtained at different stages. Good results were obtained for the operation of a temperature control circuit applied to a gas sensor system using two different methods.

8. Acknowledgements

This work was financed by CONACYT through the project number 57429. The authors thanks to Oliverio Arellano Cárdenas for his help in figures edition and formatting.

9. References

- Afridi, M. Y.; Suehle, J. S.; Zaghloul, M. E.; Berning, D. W.; Hefner, A. R.; Cavicchi, R. E.; Semanick, S.; Montgomery, C. B. & Taylor, C. J. (2002). A monolithic CMOS microhotplate-based gas sensor system. *IEEE Sensors Journal*, Vol.2, pp. 644-655, ISSN 1530437X.
- Barretino, D.; Graf, M.; Song, W. H.; Kirstein, K. U.; Hierlemann A. & Baltes, H. (2004). Hotplate-based monolithic CMOS microsystem for gas detection and material characterization for operating temperatures up to 500°C. *IEEE Journal of Solid-State Circuits*, Vol.39, pp. 1202-1207, ISSN 0018-9200.
- Cerdà, J.; Manzano, J.; Arbiol, J.; Cirera, A.; Puigcorbè, J.; Vilà, A.; Sabaté, N.; Gràcia, I.; Cané, C. & Morante, J. R. (2006). Micromachined twin gas sensor for CO and O₂ quantification based on catalytically modified nano-SnO₂, *Sens. and Act. B: Chem.*, Vol.114, pp. 881-892, ISSN 09254005.
- Fedder, G. K. (2005). CMOS-Based sensors. *Proceedings of the 4th IEEE Conference on Sensors Oct. 30-Nov. 3 2005, IEEE*, pp. 125-128, ISBN 0780390563, Irvine, CA, U.S.A. Oct. 30 - Nov. 3, 2005.
- Goering, R. (2004). Matlab® Edges Closer to Electronic Design Automation World. In: *EE Times*. Last Accessed: Feb. 8, 2011. Available from: <http://www.eetimes.com/electronics-news/4050334/Matlab-edges-closer-to-electronic-design-automation-world>
- Hsu, T. R., (2002), *MEMS & Microsystems* 1st Ed., Mc Graw Hill, ISBN 0-07-239391-2, New York, NY, U.S.A., 2002.
- Muñoz, J. S., Valencia, R. and Nieto, C. (2008). COMSOL and MATLAB Integration to Optimize Heat Exchangers Using Genetic Algorithms Technique, *Proceedings of COMSOL Conference 2008*, Boston, U.S.A, 2008.
- Ogata, K., (1999), *Problemas de Ingeniería de control utilizando Matlab® 1ª Ed.*, Prentice Hall Iberia, ISBN 84-8322-046-6, Madrid, España, 1999.